THE RECOGNITION AND TRACKING OF SEVERE CONVECTIVE CLOUD FROM IR IMAGES OF GMS①

Bai Jie (白 洁), Wang Hongqing (王洪庆) and Tao Zuyu (陶祖钰)

Laboratory for Severe Storm Research, Department of Geophysics, Peking University, Beijing 100871

Received 24 July 1995, accepted 25 December 1995

ABSTRACT

It is very important to locate and track weather systems which cause severe calamity, such as severe convective clouds (SCC), in nowcasting. In this paper the recognition and tracking of SCC is studied with GMS IR images using computer image techniques. As an IR image preprocessing, a SCC filtering algorithm is put forward that combines a segment smoothing filtering and a removal procedure by thresholds. To the filtered SCCs the T algorithm and IP algorithm of contour coding method are applied to extract the contour line and its initial point. The description of SCCs includes four characteristic quantities, i. e. center of gravity, cloud size, moment invariant M and R-shaped descriptor. Pattern recognition and pattern matching techniques are used to track the SCCs. Two procedures of rough and fine matching are given. The former procedure include the setting of searching area and recognition of area and the latter is composed by the matching of shape descriptor R and moment invariant M and the analysis of correlative brightness temperature analysis.

Key words: pattern recognition, pattern matching, recognition and tracking of severe convective cloud

I. INTRODUCTION

The tracking and forecast of severe convective clouds (SCCs) is one of the most important items in nowcasting. The destructive weather caused by SCCs is appearing most frequently, inflicting most serious calamity and thus puzzling the forecaster with the greatest difficulty. It is therefore significant to have good tracking and forecast of SCCs. Information contained in the observations by remote-sensing satellites and detecting radars, available to the user in the form of image, have not been utilized to the utmost. The part of satellite images or radar echoes a forecaster can now use is nothing more than direct dependence of his unaided eye to judge the cloud motion, being both less objective and quantitative. With the increasing development in recent years of pattern recognition and matching in the computer image technique, it is now possible for us to process the satellite images so that the statistical, shape and texture features are described, and automatic tracking methods are developed further on.

There are a lot of works in cloud motion in recent years. Fujita, Bradbnry and Murino et al. (1968) uses animated cartoon technique to judge the cloud motion artificially. McIDAS (a Man — computer Interactive Data Access System) produced by Smith (1975) et al. enables derivation of the motion of a cloud cluster following the correlative matching coefficient with the cursor-designated center by the operator on the computer screen and calculation of the cloud motion by matching correlation coefficient. SATS (SRI automatic tracking system) is one that makes it possible to track clouds with the

① This study was supported by the National Natural Science Foundation of China, No. 49405060 and No. 49675269.

characteristic quantity extracted (Endlish, Wolf and Hall et al., 1974; Hall, Endlish and Wolf et al., 1977). Arking (1978) makes a Fourier Transformation of cloud images before estimating the cloud motion by Fourier phase difference.

As it progresses into the 1980's, the research overseas was dominated by the method of multiple satellites and channels to recognize and track the cloud motion. The research in this respect in China has started late, now mostly in the testing stage, though much more work has been done regarding echo tracking by radar images relative to that by satellite cloud imagery and considerable constructive achievements have been obtained, such as Zhao and Tang (1989), Tang and Li (1989) and Tang, Zhou and Wu (1994). Their study include the application of R-shaped descriptor as well as the correlation coefficient, correlative brightness temperature and moment invariant in strong radar echoes for cloud tracking. With the successive clustering technique and sequential spotting method, Deng and Zhang (1989) use a clustering factor consisting of the center and brightness of echoes to track the motion of strong echo zone. Though some similarity exists between the tracking of radar echo cell and that of satellite image, considerable difference is also apparent. In some way, the latter is much more difficult, especially when it comes to the filtering and description of the cloud cluster.

Ⅱ. THE RECOGNITION AND TRACKING OF SCC

1. *Processing of IR image data*

The IR images used in this work are regional ones taken from full-resolution, circular GMS pictures provided by the studio of the Geophysics Department, Peking University. As the research covers mainly the east Asian low-latitudes, the original IR images have been transformed through the Mercator projection (Fig. 1).

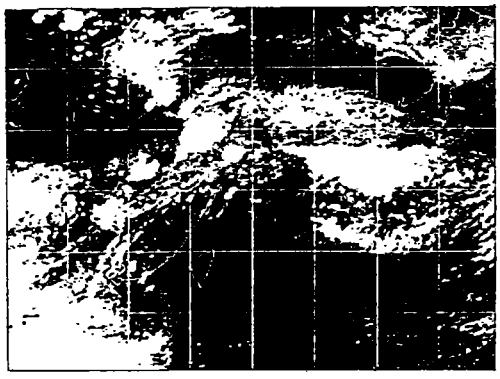

Fig. 1. An IR image transformed through the Mercator projection at 06 UTC, 1 Aug 1993.

It is inevitable for an IR satellite image to expose to some disturbance and noise which lower the quality of the cloud image. Hence, a method of nine-point smoothing algorithm is used here to remove the noise disturbance.

The smoothing equation for derivation of the mean is

$$X_{m,n}=\frac{1}{(2k+1)\cdot(2k+1)}\sum_{i=-k}^{k}\sum_{j=-k}^{k}x(i+m,j+n)$$

where k is the segment scale at point (m, n). If $k=1$, the segment is 3×3; if $k=2$, the segment is 5×5.

The information from the image edge tends to be indeterminate with larger k. For the purpose of retaining as much the edge information as possible, $k=1$ in this paper.

2. *Recognition of SCC*

In addition to SCCs, There are also some smaller-scale SCCs and non-SCC clusters or regimes in an IR satellite image that is smoothed and filtered. They are not only less important for nowcast but also distracting in the processing, recognition and tracking of IR images. The segment-smoothing filter algorithm and threshold-eliminating algorithm are used to separate the SCC from IR satellite image for extraction of the SCC contour line and record of its initial point using the T and IP algorithms in the outline coding method in computer image processing.

1) SEGMENT SMOOTHING FILTER ALGORITHM

A dual-smoothed picture is first created by computing the average brightness twice in a window encompassing 11×11 pixel points following the equation above in which $k=5$. Then, the greyness of each pixel point between the raw image and smoothed image is compared. If the greyness for the raw image is brighter than the latter, it is retained, and it is eliminated otherwise (Endlish, Wolf and Hall et al., 1971). As a result, some regimes of cloud besides the treated SCCs are let through on to the second stage, then the threshold-eliminating algorithm is used to circle them off, based on the fact that the cloud-top temperature is warmer than that of a SCC.

2) THRESHOLD-ELIMINATING ALGORITHM

(1) Set the threshold for IR brightness temperature G, and use it for elimination of non-SCCs slipped through from the filtering in Section 2. 1. The procedure circles off most of non-SCCs. The value of the threshold G, set at 180 by experiment in this paper, is based on the observation that the TBB of a SCC is much colder than other clusters or ground surface. The treatment rounds off the boundary of SCCs by some extent.

(2) Set the area threshold S_0. When applied, small and scattered clouds with area $S<S_0$ are eliminated.

In the SCCs remaining after the treatment in Sections 2. 1 and 2. 2, some hollows are found within the boundary of larger-sized clouds, which is supposed to be caused by higher individual threshold for IR brightness temperature and segment-smoothing algorithm applied. These SCCs are made complete by filling up the hollows with data of raw cloud images after extraction of cluster outlining contour with the T and IP algorithms in Sections 2. 3. (Fig. 2)

Fig. 2. Severe convective clouds separated from Fig. 1.

3) EXTRACTION OF SCC OUTLINING CONTOUR

The shape of cloud is described by the shape of its outlining contour and parameters like the center of gravity, area of cloud etc. can further be determined by the contour extracted. In this paper, the contour coding method in the computer image processing technique is used to extract the contour line (see the detailed algorithm in Gonazalez and Wintz, 1983) and mark out the initial point of boundary, re-

spectively by T algorithm of sequential series and IP contour initiating algorithms.

3. *Description of SCCs*

For the marked SCCs, the following statistic and characteristic shape quantities, the center of gravity, characteristic area, moment invariant M and shape descriptor R are used, to describe the SCCs.

1) CENTER OF GRAVITY AND CHARACTERISTIC AREA OF SCC

The center of gravity in a SCC can be used to express where the SCC locates by

$$\bar{x} = \sum_{i=1}^{N} x_i \cdot G_i / \sum_{i=1}^{N} G_i, \qquad \bar{y} = \sum_{i=1}^{N} y_i \cdot G_i / \sum_{i=1}^{N} G_i,$$

where x_i, y_i is the mesh coordinate of the pixel points in the image, G_i is the greyness of the pixel point.

The total of the pixels in a SCC is the characteristic area, depicting the size of the SCC.

2) MOMENT INVARIANT M

For a two-dimensional IR brightness temperature field $G(i, j)$, the central moment is

$$\mu_{p,q} = \sum_{i=0}^{M} \sum_{j=0}^{N} (i - \bar{i})^p \cdot (j - \bar{j})^q \cdot G(i,j)$$

where $\bar{i} = \frac{m_{10}}{m_{00}}, \bar{j} = \frac{m_{01}}{m_{00}}, m_{pq} = \sum_{i=0}^{M} \sum_{j=0}^{N} i^p \cdot j^q \cdot G(i,j), p, q = 0,1,2,\cdots\cdots M,N$; M, N are the horizontal and vertical scale of the SCC, respectively; i, j the position coordinates of the mesh; $G(i, j)$ the value of brightness temperature of the pixel point. The central moment μ_{pq} is physically depicting the distribution of the field of brightness temperature relative to the center of gravity.

$$\eta_{pq} = \frac{\mu_{pq}}{\mu_{00}^{\gamma}},$$

where $\gamma = \frac{p+q}{2} + 1$.

The following 7 moment invariants are obtained using two and three standardized central moments:

$$\begin{aligned}
\Phi_1 &= \eta_{20} + \eta_{02} \\
\Phi_2 &= (\eta_{20} - \eta_{02})^2 + 4\eta_{11}^2 \\
\Phi_3 &= (\eta_{30} - 3\eta_{12})^2 + (3\eta_{21} - \eta_{03})^2 \\
\Phi_4 &= (\eta_{30} + \eta_{12})^2 + (\eta_{21} + \eta_{03})^2 \\
\Phi_5 &= (\eta_{30} - 3\eta_{12})(\eta_{30} + \eta_{12})[(\eta_{30} + \eta_{12})^2 - 3(\eta_{21} + \eta_{03})^2] \\
&\quad + (3\eta_{21} + \eta_{03})(\eta_{21} + \eta_{03})][3(\eta_{30} + \eta_{12})^2 - (\eta_{21} + \eta_{03})^2] \\
\Phi_6 &= (\eta_{20} - \eta_{02})[(\eta_{30} + \eta_{12})^2 - (\eta_{21} + \eta_{03})^2] \\
&\quad + 4\eta(\eta_{30} + \eta_{12})(\eta_{21} + \eta_{03})]
\end{aligned}$$

$$\Phi_7 = (\eta_{21} - 3\eta_{03})(\eta_{30} + \eta_{12})[(\eta_{30} + \eta_{12})^2 - 3(\eta_{12} - \eta_{03})^2] - (\eta_{30} - 3\eta_{12})(\eta_{21} + \eta_{03})[3(\eta_{30} + \eta_{12})^2 - (\eta_{12} + \eta_{03})^2]$$

Researches of the science of image (Gonzalez and Wintz, 1983; Tang and Li, 1989) have shown that the set of moment invariants above is well conservative for the image of the same object at intervals of mild length, yet assigning contrasting difference for different objects.

3) SHAPE CENTER AND SHAPE DESCRIPTOR R OF SCC

In Section 2. 3, the cloud boundary is in turn marked down as $f = \{f_0, f_1, f_2, f_3, \cdots, f_i, \cdots, f_{N-1}\}$, where f_0 is the first point of cloud contour line, and $f_i = x_i + \bar{j}y_i, (i = 0,1,2,\cdots,N-1)$.

The shape center of enclosed cluster contour is $\bar{f} = \frac{1}{N}\sum_{i=0}^{N-1} f_i, \bar{x} = \frac{1}{N}\sum_{i=0}^{N-1} x_i, \bar{y} = \frac{1}{N}\sum_{i=0}^{N-1} y_i$ and the distance between the shape center and its contour point is $d_i = |f_i - \bar{f}| = \sqrt{(x_i - \bar{x})^2 + (y_i - \bar{y})^2}$

The 2-dimensional coordinate of boundary points can be expressed by the distance sequence in $d = \{d_0, d_1, d_2, \cdots\cdots d_i, \cdots\cdots d_{N-1}\}$

A group of R-shaped descriptor is obtained with standardization by performing R transformation to the distance sequence as in

$$d^R_{(m+2ns)} = \left| d^{(R-1)}_{m+2ns} + d^{(R-1)}_{m+(2n+1)s} \right|_{m=0 \quad n=0}^{s-1 \quad t-1}$$

$$d^R_{m+(2n+1)s} = \left| d^{(R-1)}_{M+2ns} - d^{(R-1)}_{m+(2n+1)s} \right|_{m=0 \quad n=0}^{s-1 \quad t-1}$$

where $N = 2^M, R = 1,\cdots,M, s = 2^{M-R}, T = 2^{R-1}$.

The R transformation possesses the constant quality of circulating shift, which ensures that the characteristic quantities extracted from closed cloud clusters would not change with the initial point in the contour line. The work (Lu, Ma and Wu, 1987) shows that the R descriptor derived by the group of characteristic quantities is only related to the shape of the boundary in targets of concern, in addition to properties of horizontal dislocation, rotation and shrinking/enlarging without changes in shape. It can be used to track SCCs.

4. *Tracking of SCCs*

With the use of the characteristic quantities described in the preceding section for a given sheet of cloud image, SCCs at a different time in sequence can be identified following the principle of similarity. Multi-level control is exercised through methods of pattern recognition and matching so that accurate recognition of movement of a target cloud cluster is eventually possible for any two consecutive time. The multi-level control includes two procedures. First, a rough comparison and analysis is done for selection of SCCs. Then, a fine process follows. Both procedures are based on the technique of pattern recognition.

1) ROUGH COMPARISON AND ANALYSIS

(1) Setting of areas searched

The possible maximum speed at which a cloud cluster moves at each level is based to determine corresponding maximum distance dislocated and maximum radius of search for cluster tracking. The setting increases the processing of computers. Whether or not the tracked SCC is within the area is judged by the difference in barycentric range between the tracked and targeted SCCs.

The difference in barycentric range $\triangle d$ between the target SCC and all SCCs in a successive image is computed. For an area of search, assume the maximum scale as L and select those with $\triangle d < L$.

(2) Recognition of area

For a cloud cluster selected by the barycentric range, the area S_2 is derived and compared with that of the target cloud cluster to arrive at the standardized area distance $\triangle S$ as in

$$\triangle S = \frac{|S_2 - S_1|}{\max\{S_1, S_2\}},$$

and the cloud cluster is selected in which $\triangle S$ is smaller than a given area threshold Cs. The selected cloud cluster determined by the rough process is then analyzed in the following fine process for clusters similar to the target cluster.

2) FINE COMPARISON AND ANALYSIS

This process is composed by the matching of R-shaped descriptor and moment invariant, and the analysis of correlative coefficient of brightness temperature. The match of the first two factors reflect the boundary shape of the cloud cluster and distribution of the field of brightness temperature relative to the barycenter, respectively. Similarly, the last factor is appropriate for analysis of the matchness among various cloud clusters in uneven flow field.

(1) Matching of R-shaped descriptor

From the cloud cluster roughly selected, a R-shaped descriptor R_i (t_2) is extracted so that $\triangle R$ is computed using R_i (t_1), another descriptor for the target cluster by

$$\triangle R = \sum_{i=0}^{N-1} |R_i(t_2) - R_i(t_1)|$$

where i=0, 1, ···, N. When $\triangle R < C_r$, the threshold given, the cluster is included in the selection. Otherwise, it is circled off from the candidates. The descriptor match well reflects the match between large-sized SCCs.

(2) Matching of moment invariant

With the matching process at the previous level, the moment invariant Φ_2 is computed for the selected cloud cluster and the standardized difference $\triangle\Phi$ further computed between it and the moment invariant Φ_1 for the target cluster by

$$\triangle\Phi = \frac{|\Phi_2 - \Phi_1|}{\max\{\Phi_1, \Phi_2\}}.$$

If $\triangle\Phi$ is less than the given threshhold C_Φ, the cloud cluster is selected for next level of candidates, or, it is removed for good.

(3) Analysis of correlative brightness temperature

For k cloud clusters selected, the analysis of correlation-brightness is applied to identify the cluster in the candidates that is maximally correlated to the brightness-temperature coefficient, with affirmation that it is just the same as the target cluster in a successive cloud image. The coefficient is derived assuming that there are two cloud clusters respectively locating at (I, J) and (I', J'), and a template domain is composed by $m \times n$ pixel points around its center in which m and n are the maximum scale in the horizontal and vertical directions of the cluster. Take the pixel points in the template domains as sample with a greyness of $G(I, J)$ and the respective sample matrixes are expressed by

$$G_1(I,J) = \begin{bmatrix} G_1(1,1) & G_1(1,2) & \cdots & G_1(1,n) \\ & \cdots\cdots & & \\ G_1(m,1) & G_1(m,2) & \cdots & G_1(m,n) \end{bmatrix},$$

$$G_2(I,J) = \begin{bmatrix} G_2(1,1) & G_2(1,2) & \cdots & G_2(1,n) \\ & \cdots\cdots & & \\ G_2(m,1) & G_2(m,2) & \cdots & G_2(m,n) \end{bmatrix}$$

The correlation coefficient between the sample matrixes is

$$\gamma_{(I,J)}^{(I',J')} = \frac{\sum_{i=1}^{m}\sum_{j=1}^{n}(G_1(i,j) - \overline{G}_1) \cdot (G_2(i,j) - \overline{G}_2)}{\{\sum_{i=1}^{m}\sum_{j=1}^{n}(G_1(i,j) - \overline{G}_1)^2 \cdot \sum_{i=1}^{m}\sum_{j=1}^{n}(G_2(i,j) - \overline{G}_2)^2\}^{1/2}}$$

where

$$\overline{G}_1 = \frac{1}{m \cdot n}\sum_{i=1}^{m}\sum_{i=1}^{n}G_1(i,j), \qquad l = 1,2$$

For all particles within a cloud cluster, the brightness temperature is averagely weighted at $\overline{G} = \sum_{i=1}^{m}\sum_{i=1}^{n}a_{i,j} \cdot G_1(i,j)$ where $a_{i,j}$ is the weighting factor of brightness temperature (taken to be $\frac{1}{m \cdot n}$ in this work). $\overline{G}$ is the average weighted brightness temperature of the cloud cluster. By taking $G_1(I, J)$ and $G_2(I', J')$ as the average brightness temperature of cloud clusters $\overline{G}(I,J)$ *and* $\overline{G}_2(I',J')$, $k_{(I,J)}^{(I,J)} = \left|\frac{G_1(I,J)}{G_2(I',J')} - 1\right|$ can be assumed as the factor of brightness temperature, reflecting in effect the difference in brightness temperature between the clusters.

In order to accurately keep track of the SCC, the correlation coefficient γ is maintained as large as possible and the factor of brightness temperature as small as possible. So let $q = \gamma - k$, in which q is the correlation coefficient of brightness temperature. Individual q_i $(i = 1, 2, \cdots, k)$ is computed for k cloud clusters and the cluster with maximum q_i is selected as the one that best matches the target cluster.

5. *The discussion of results of SCC tracking*

Following the method mentioned above, a tracking experiment is performed with IR satellite images at interval of 1 h 00 — 06 UTC, 1 August 1993 and the results are presented in Fig. 3. It is known in the figure that averagely more than half of the SCCs in a cloud image are tracked while the rest not tracked for stopping short of the criteria. 90%

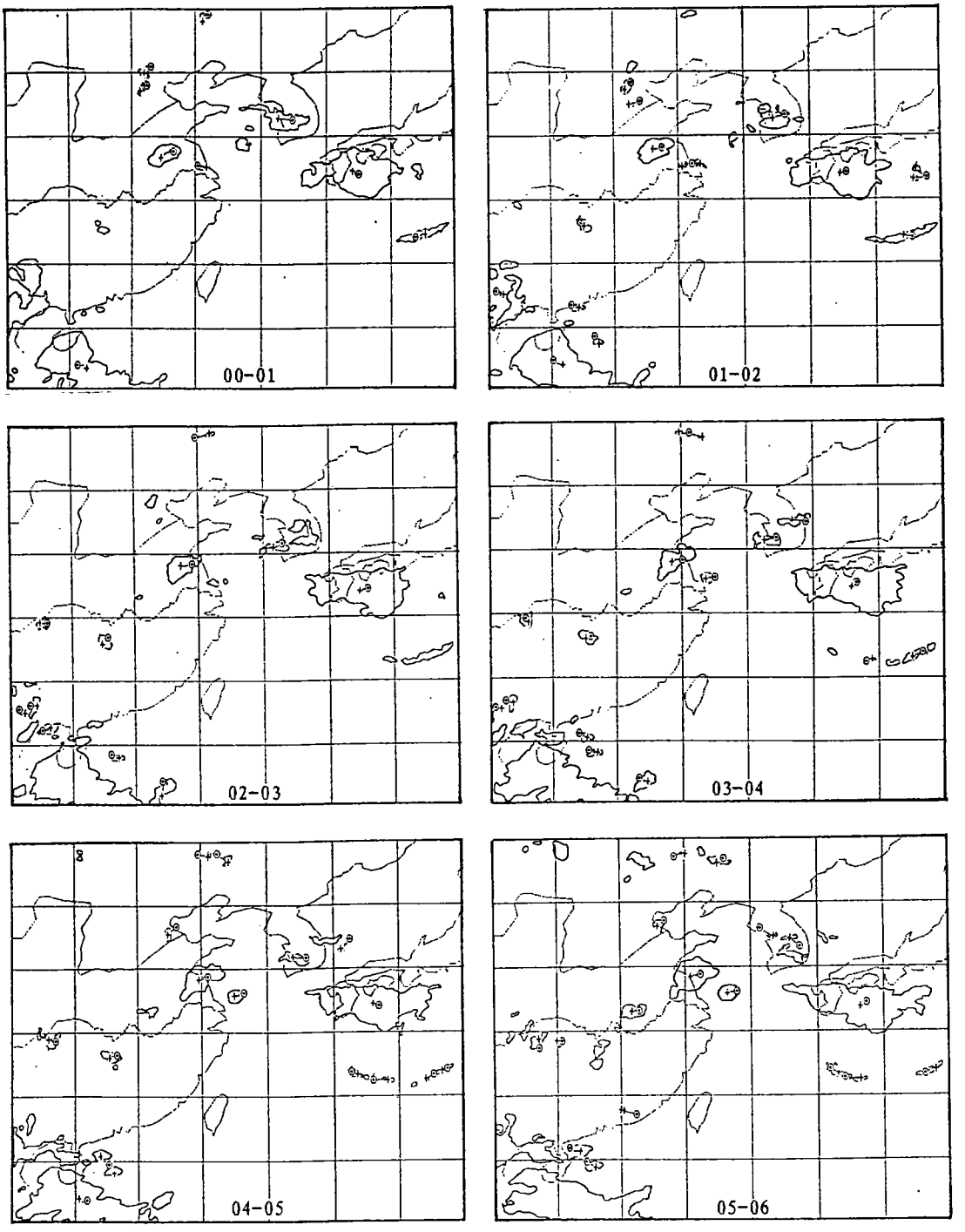

Fig. 3. Results of SCCs tracing experiments from 00 UTC to 06 UTC 1 August 1993. (+ The barycenter in SCCs in Hour 1; ⊙ the barycenter in SCCs in Hour 2; — the track of motion.)

of the cloud clusters tracked are accurate, suggesting a basically successive application of the method offered in this paper. One such example is the revelation of westward (eastward) movement of SCCs in the equatorial easterlies over the South China Sea (westerlies north of the western Pacific subtropical high). Two reasons are behind why other SCCs are not tracked. One is the time interval used. It is too long to keep track of the SCCs with irregular and variable shape or small size, i. e. those over the Korean Peninsula and the Hainan Island. If images at 30-minute intervals are used instead, much more SCCs will be tracked. The other reason for the failure of tracking is that the SCCs generate, decay or develop quickly, e. g. those over the Korean Peninsula. About 10% of the cloud clusters are lost in the tracking, mostly attributable to mergence or spliting during the motion in addition to fast development of the SCCs.

Ⅲ. CONCLUSIONS

a. An algorithm combining segment-smoothing filtering and removal by threshold is suggested so that SCCs are effectively isolated from IR images, whose boundary shape is extracted accurately with the procedure of contour coding that is featured by light and fast computation.

b. A SCC is described by the barycenter, characteristic area, moment invariant M and R-shaped descriptor. With accuracy and rationality, they depict the characters and properties of SCCs.

c. Two pattern matching processes are designed, namely, the rough and fine comparison and analyses. The former process is made up of two steps, the setting of a searching area and the recognition of area, while the latter by three components of the matching of the R-shaped descriptor and moment invariant, and the analysis of correlative coefficient of brightness temperature. The fine matching process proves a success in the tracking experiment shown, because it takes account of both the external and physical characteristics of the SCCs.

Only the IR images are used in this work, leaving the other parts of satellite data, the visible and moisture data virtually intack. How to apply all of the three kinds of data in the tracking of SCCs is the goal in the research to come. For an accurate tracking, physical mechanisms and conceptual models in the synoptics and atmospheric physics are needed additionally. For example, it has been found (Tao, Wang, Bai et al., 1995) that a MCC with large area and lateraly gradient attracts a small-sized convective cell around it. It provides a useful concept for coping with the merged SCCs in tracking.

REFERENCES

Arking A, Lo R C, Rosenfield A, 1978. A furrier approach to cloud motion estimation, *J. Appl. Meteor.*, 17: 735—744.

David J H, Endlish R M, Wolf D E et al., 1977. Experiments in automatic cloud tracking using SMS-GOES data, *J. Appl. Meteor.*, 16: 1219—1230.

Deng Yong, Zhang Peichang, 1989. Nowcasting the course of severe convective weather by using the most intensive echo image in the digital radar cylinder, *J. Nanjing Inst. Meteor.* 12 (4): 405—414 (in Chinese).

Endlish R M, Wolf D E, Hall D J et al., 1971. Use of a pattern recognition technique for determining cloud motions from sequences of satellite photographs, *J. Appl. Meteor.*, 10: 105—117.

Fujita T, Bradbnry D L, Murino C et al., 1968. A study of mesoscale cloud motions computed from ATS-I and terrestrial photographs, SMRP Res. Pap., 71, University of Chicago, 25pp.

Gonazalez R C, Wintz P, 1983. Digital image processing, Academic Press, 247—293, 370—381. (in

Chinese)

Lu Xinru, Ma Jun, Wu Chengke, 1987. A shape analytical method of two dimensional objects, *J. China Inst. Communications*, 8 (3): 61—67 (in Chinese).

Smith E A, 1975. The McIDAS system, IEEE Trans. Geosci. Electron GE-13, 123—136.

Tang Dazhang, Li Li, 1989. A new characteristics of tracking radar echo-moment invariant, *J. Nanjing Inst. Meteor.*, 12 (3): 1—8 (in Chinese).

Tang Dazhang, Zhou Yongmei, Hu Mingbao, 1994. Two radar echo tracking methods and comparison between their accuracies, *Quarterly J. Applied Meteor.*, 1 (3): 305—311 (in Chinese).

Tao Zuyu, Wang Hongqing, Bai Jie et al., 1995. A case of mesoscale convective complex evolving into a vortex. *Acta Meteorologica Sinica*, 9 (2): 184—189.

Zhao Qingyun, Tang Dazhang, 1988. Method study for tracking radar echoes (Ⅱ) *J. Nanjing Inst. Meteor.*, 11 (2): 197—207 (in Chinese).